CrystEngComm

View Online / Journal Homepage
Dynamic Article Links

Cite this: DOI: 10.1039/c2ce25495f

www.rsc.org/crystengcomm

PAPER

Examining the robustness of a theophylline cocrystal during grinding with additives†‡

Heba Abourahma,*[a] Jennifer M. Urban,[a] Nicole Morozowich[b] and Benny Chan[a]

Received 4th April 2012, Accepted 23rd April 2012
DOI: 10.1039/c2ce25495f

The robustness of theophylline-*p*-hydroxybenzoic acid cocrystal (TP·*p*HBA) while grinding with additives in the solid state was evaluated through a series of solvent-drop grinding experiments with coformers containing various functional groups. Powder X-ray diffraction was used to qualitatively analyse the powders after grinding and identify the species present. The TP·*p*HBA cocrystal was found to be robust in the presence of benzoic acid (BA), *p*-nitrobenzoic acid (*p*NBA), *p*-(*N*,*N*-dimethylamino)benzoic acid (dMABA), *m*-hydroxybenzoic acid (*m*HBA), *p*-nitrophenol (*p*NP), hydroquinone (HDQ) and benzamide (BZA), but it disintegrates in the presence of salicylic acid (SA), 3,5-dinitrobenzoic acid (dNBA), acetamide (ACA) and melamine (MLM).

Introduction

Pharmaceutical cocrystals,[1,2] cocrystals comprised of at least one active pharmaceutical ingredient (API), have been shown to improve a number of physical properties of the API, including poor solubility,[3–8] poor hydration stability,[9,10] poor compressibility[11] and poor thermal stability.[7,12,13] Since pharmaceutical cocrystals offer great potential to address the limitations of certain APIs, they have gained a lot of interest in recent years.[14–16] However, if a promising pharmaceutical cocrystal were to be formulated into a tablet, how likely is it that it will stay intact in the presence of additives, excipients and binding materials that go into making the drug tablet? Grinding has been shown to effect chemical transformations in the solid state,[17,18–20] as well as cause cocrystal disintegration.[21] So how robust is a pharmaceutical cocrystal during grinding with additives in the solid state? This study addresses the question by evaluating the robustness of a pharmaceutical cocrystal containing theophylline, a muscle relaxant used in asthma medications. Over 40 cocrystals of theophylline have been reported in the literature[22] making it an excellent model compound for our study.

The cocrystal selected for this study is theophylline-*p*-hydroxybenzoic acid, TP·*p*HBA. It can be synthesized readily in high yield and purity and has been characterized by single crystal X-ray crystallography,[22] which provides insight into the hydrogen bonding interactions sustaining the cocrystal. The crystal structure of TP·*p*HBA, shown in Fig. 1, reveals that each TP molecule interacts with two *p*HBA molecules *via* supramolecular synthon[23] I ($R_2^2(9)$ motif)[24] and synthon II (D(2) motif).

The selected competing coformers and abbreviations, shown in Fig. 2, are: *p*-(*N*,*N*-dimethylamino)benzoic acid (dMABA), benzoic acid (BA), *p*-nitrobenzoic acid (*p*NBA), *o*-hydroxybenzoic acid (salicylic acid, SA), *m*-hydroxybenzoic acid (*m*HBA), 3,5-dinitrobenzoic acid (dNBA), *p*-nitrophenol (*p*NP), hydroquinone (HDQ), benzamide (BZA), acetamide (ACA) and melamine (MLM). Five of the 11 coformers are known to form cocrystals with TP, namely BA,[25] *p*NBA,[25] dNBA,[22] SA[22] and *p*NP,[26] and the latter two were characterized by single crystal X-ray diffraction (CSD refcodes KIGLES and TOPPNP, respectively). All selected coformers are capable of interacting with theophylline through one of the synthons illustrated in

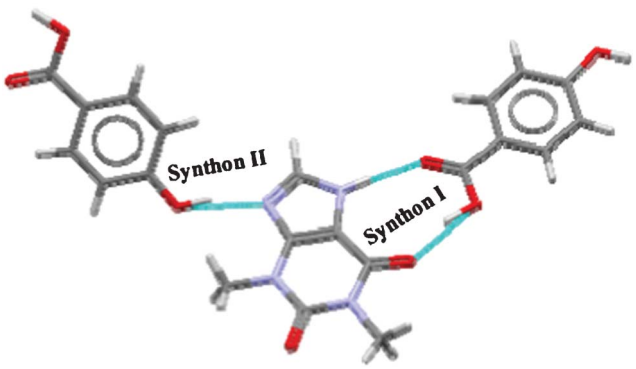

Fig. 1 Crystal structure of TP·*p*HBA (CSD refcode KIGLOC).

[a]*Department of Chemistry, The College of New Jersey, 2000 Pennington Rd, Ewing, NJ, USA. E-mail: abourahm@tcnj.edu; Fax: 609-637-5157; Tel: 609-771-3302*
[b]*Department of Chemistry, Penn State University, 104 Chemistry Building, University Park, PA 16802, USA*

† Electronic supplementary information (ESI) available: Characterization data of TP·ACA and TP·MLM·DMSO including CIF, PXRD, ^{1}H NMR, DSC and IR. In addition, complete PXRD data for all reactions described herein and some DSC data are included. CCDC reference number 879008. For ESI and crystallographic data in CIF or other electronic format see DOI: 10.1039/c2ce25495f

‡ The authors acknowledge The College of New Jersey for financial support (startup funds), Dr Christopher Cahill and Nicholas Deifel for crystal data collection and Professor Christer Aakeröy for his invaluable feedback and the many insightful and fruitful discussions during the preparation of this manuscript.

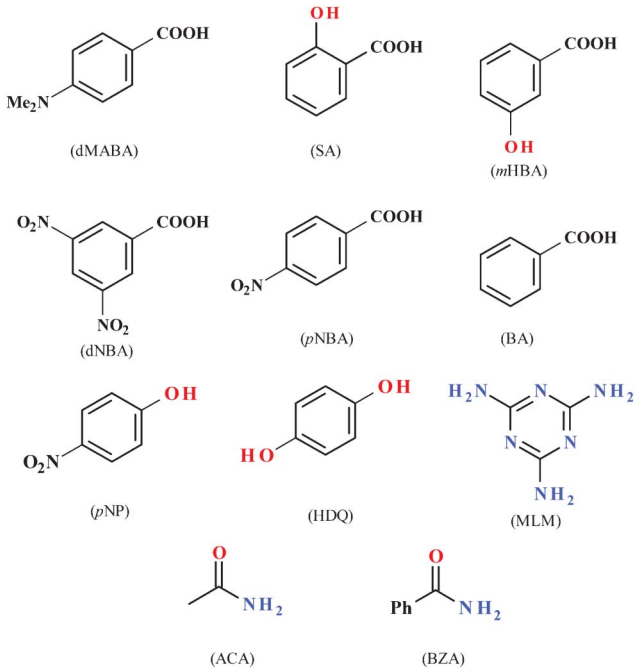

Fig. 2 Chemical structure and abbreviation of coformers employed in evaluating the robustness of TP·*p*HBA.

Fig. 1, in addition to hydrogen bonding to the second carbonyl functionality in TP. The benzoic acid coformers were selected to have varying competency of hydrogen bonding.

Two general types of experiments, outlined in Fig. 3, were conducted in this study: (A) competition experiments involved grinding TP·*p*HBA with a stoichiometric amount of a coformer to see if the cocrystal stays intact; and (B) selectivity experiments involved grinding TP with a stoichiometric binary mixture of *p*HBA and a second coformer to determine the affinity of TP for *p*HBA. Solvent-drop grinding (SDG) was utilized in these experiments since it has been shown to enhance reaction kinetics significantly and improve yields.[20,27] The effect of grinding time on the reaction was examined by sampling the ground mixture after 20, 40 and 60 min. Powder X-ray diffraction was used to qualitatively analyse the powders after grinding and identify the species present. No quantitative measurements were conducted in this study.

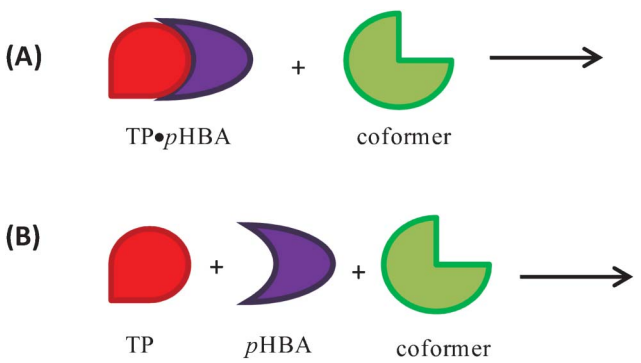

Fig. 3 Two general types of experiments conducted: (A) competition experiment and (B) selectivity experiment.

Results

Table 1 gives an overview of the results obtained in this study. The TP·*p*HBA cocrystal is found to be robust in the presence of 7 coformers (Table 1, a–b), but disintegrates in the presence of 4 coformers (Table 1, c–e). Grinding time does not appear to have an effect on the composition of the ground product, qualitatively. During the course of this study, 2 new theophylline cocrystals were discovered, namely TP·ACA and TP·MLM·DMSO, and fully characterized by PXRD, IR, DSC and ^{1}H NMR. TP·MLM·DMSO was additionally characterized by single crystal X-ray crystallography and the complete characterization data for both cocrystals is included in the electronic supplementary information (ESI). †Details of the competition and selectivity experiments evaluating the robustness of TP·*p*HBA are described herein.

Competition experiments

Competition experiments were conducted to evaluate the robustness of TP·*p*HBA in the presence of a competing coformer. Fig. 4 shows a typical result from the solvent-drop grinding (SDG) of TP·*p*HBA with a stoichiometric amount of a coformer, in this case BZA.

The PXRD pattern of the product shows that TP·*p*HBA stays intact in the presence of BZA and no displacement of *p*HBA by BZA is observed. Indeed, this was observed for 4/11 coformers used in this study (coformer = BZA, BA, *p*NP and HDQ), as illustrated in the following equation:

$$\text{TP·}p\text{HBA} + \text{coformer} \rightarrow \text{TP·}p\text{HBA} + \text{coformer}$$

In the case of *m*HBA, dMABA and *p*NBA, the cocrystal stays intact; however, each of the coformers undergoes a phase change, as determined by PXRD. The outcome from these experiments is schematically illustrated in Table 1 (b).

When stoichiometric amount of ACA is ground with TP·*p*HBA, the cocrystal partially disintegrates. PXRD data (Fig. 5) shows that a mixture of TP cocrystals is present, namely

Table 1 A summary of the results obtained from experiments evaluating the robustness of TP·*p*HBA in the presence of competing coformers: (a) The cocrystal is robust and the coformer is recovered intact; (b) the cocrystal is robust, but the coformer undergoes a polymorphic change; (c) a mixture of TP cocrystals results in addition to a cocrystal of the two coformers; (d) the cocrystal disintegrates and the coformer is recovered along with TP and a cocrystal of pHBA and coformer; (e) a new phase containing all three components forms

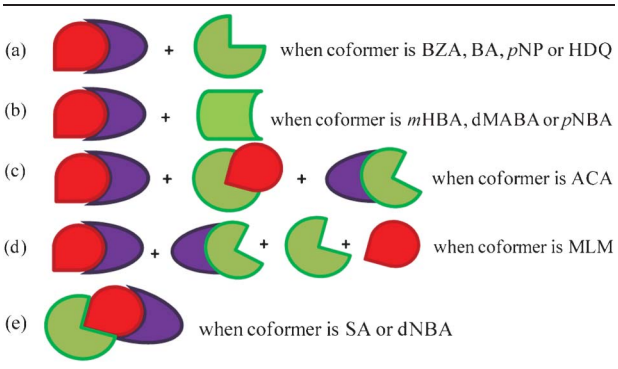

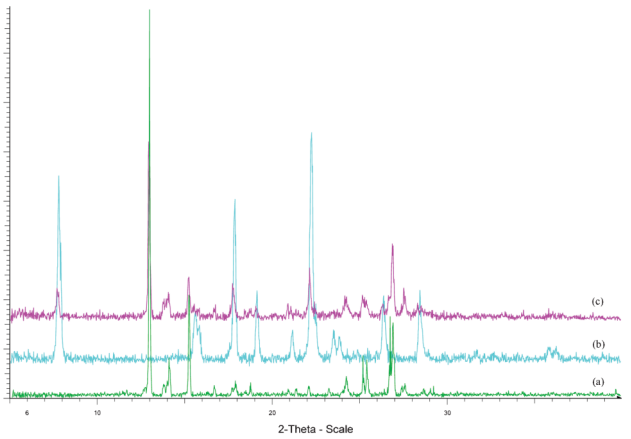

Fig. 4 PXRD data for (a) TP·*p*HBA, (b) BZA, (c) product of grinding TP·*p*HBA and a stoichiometric amount of BZA.

TP·*p*HBA and TP·ACA, in addition to a cocrystal of the two coformers, ACA·*p*HBA. The existence of the latter cocrystal was confirmed by a separate experiment in which *p*HBA and ACA were ground together and the PXRD pattern of the product was found to match that of the ACA·*p*HBA cocrystal from the above experiment. The outcome from the competition experiment with ACA is illustrated in the following equation:

$$\text{TP·}p\text{HBA} + \text{ACA} \rightarrow \text{TP·}p\text{HBA} + \text{TP·ACA} + \text{ACA·}p\text{HBA}$$

When stoichiometric amount of MLM is ground with TP·*p*HBA, the cocrystal disintegrates and a mixture of products is present according to the following equation:

$$\text{TP·}p\text{HBA} + \text{MLM} \rightarrow \text{TP·}p\text{HBA} + \text{MLM·}p\text{HBA} + \text{TP} + \text{MLM}$$

The existence of the *p*HBA·MLM cocrystal was confirmed by a separate experiment in which *p*HBA and MLM were ground together and the PXRD pattern of the product was found to match that of the MLM·*p*HBA cocrystal from the above experiment.

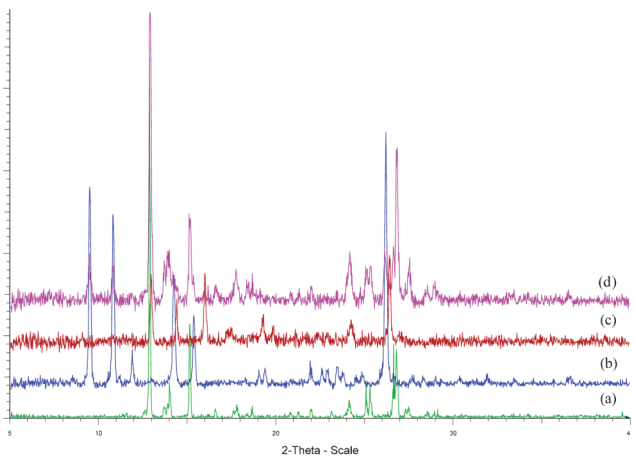

Fig. 5 PXRD data for (a) TP·*p*HBA, (b) TP·ACA, (c) *p*HBA·ACA, (d) product of the competition experiment involving TP·*p*HBA and stoichiometric amount of ACA.

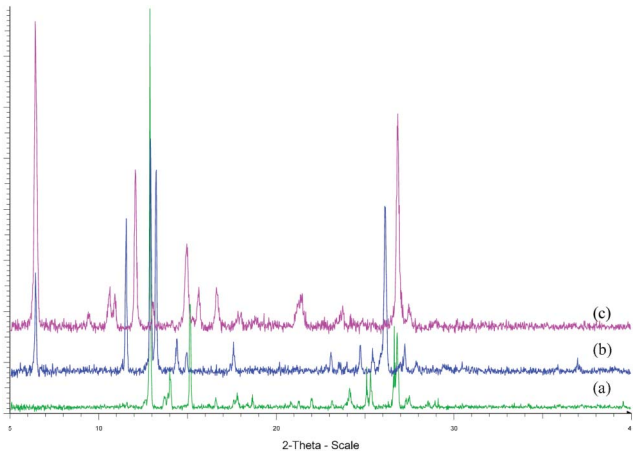

Fig. 6 PXRD data for (a) TP·*p*HBA, (b) TP·SA, (c) product of the competition experiment involving grinding TP·*p*HBA with stoichiometric amount of SA.

When a stoichiometric amount of SA is ground with TP·*p*HBA, a new phase is obtained, as determined by PXRD (Fig. 6). PXRD data of the ground product shows a unique pattern that is different from the PXRD patterns of either cocrystal; it is also different from any of the starting materials.

The same phase is obtained from solution crystallization of stoichiometric amounts of TP, *p*HBA and SA. ^{1}H NMR of the crystalline material obtained from solution revealed that the product contains all three components (TP, *p*HBA, SA) in 1 : 1 : 1 ratio. Furthermore, the DSC heating curve of the product shows a sharp endotherm at 183.5 °C, compared to the DSC heating curve of a physical mixture of stoichiometric amounts of the three compounds which shows three endotherms (ESI, Fig. S8c†). Therefore it was concluded that grinding of TP·*p*HBA with SA forms a ternary cocrystal, namely TP·*p*HBA·SA, as shown schematically in Fig. 7. A similar result is obtained when TP·*p*HBA is ground with stoichiometric amount of dNBA. A new phase, the PXRD pattern of which does not correspond to any of the cocrystals or the starting materials, is obtained and is also believed to be a ternary cocrystal. DSC experiments of the new phase compared to a physical mixture of stoichiometric amounts of the three compounds shows a sharp endotherm at 229 °C, compared to three phase transitions for the physical mixture of the three compounds (ESI, Fig S11c†). Examples of ternary cocrystals prepared by SDG have previously been reported.[28,29]

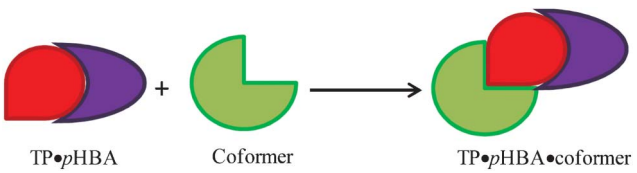

Fig. 7 Schematic representation of the competition experiment involving stoichiometric amounts of TP·*p*HBA and SA or dNBA.

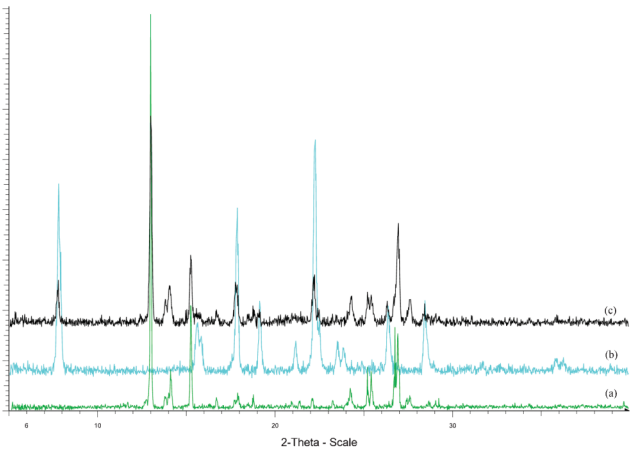

Fig. 8 PXRD data for (a) TP·*p*HBA, (b) BZA and (c) product of SDG of stoichiometric mixture of TP, *p*HBA and BZA. TP selectively cocrystallizes with *p*HBA to form a cocrystal while BZA is recovered.

Selectivity experiments

Selectivity experiments were conducted to determine the affinity of TP for *p*HBA in the presence of a competing coformer. A representative result from SDG experiment of TP with a stoichiometric mixture of *p*HBA and BZA is shown in Fig. 8. PXRD data reveals that TP selectively cocrystallizes with *p*HBA to yield TP·*p*HBA, while BZA is recovered unreacted, according to the following equation:

$$\text{TP} + p\text{HBA} + \text{coformer} \rightarrow \text{TP}\cdot p\text{HBA} + \text{coformer}$$

TP has higher affinity for *p*HBA in the presence of 7/11 coformers, namely BA, *p*NBA, dNBA, dMABA, *p*NP, HDQ, BZA, and *m*HBA. In the case of *m*HBA, dMABA and *p*NBA, TP does selectively cocrystallize with *p*HBA, but each of the coformers undergoes a polymorphic change. These results are consistent with the competition experiments involving the same coformers.

A different result is obtained when ACA is used. When TP is ground with a stoichiometric mixture of ACA and *p*HBA, it cocrystallizes with each of the coformers resulting in a mixture of TP cocrystals, namely TP·*p*HBA and TP·ACA. PXRD data confirmed the presence of both cocrystals, in addition to ACA·*p*HBA. These results are consistent with the results obtained from the competition experiment involving ACA.

Grinding TP with a stoichiometric binary mixture of *p*HBA and SA or *p*HBA and dNBA results in the same phases obtained from the competition experiment, which were identified as ternary cocrystals TP·*p*HBA·SA and TP·*p*HBA·dNBA, respectively.

Reverse experiments

To further confirm that the robustness of the TP·*p*HBA cocrystal is due to the high affinity of TP for *p*HBA and not that the cocrystal was pre-formed, we conducted experiments with selected coformers in which TP·coformer was ground with stoichiometric amount of *p*HBA. The results from experiments involving MLM and ACA are described below.

Grinding TP·MLM with stoichiometric amount of *p*HBA results in disintegration of the TP·MLM cocrystal and the formation of a mixture of TP cocrystals, in addition to MLM·*p*HBA, according to the following equation:

$$\text{TP}\cdot\text{MLM} + p\text{HBA} \rightarrow \text{TP}\cdot\text{MLM} + \text{TP}\cdot p\text{HBA} + \text{MLM}\cdot p\text{HBA}$$

Grinding TP·ACA with a stoichiometric amount of *p*HBA resulted in a mixture of TP cocrystals, in addition to ACA·*p*HBA. This is the same outcome obtained from all previously described experiments involving ACA.

Excess coformer experiments

The above-described competition and selectivity studies revealed that TP·*p*HBA is robust in the presence of a stoichiometric amount of 7 coformers and that TP selectively cocrystallizes with *p*HBA in a stoichiometric binary mixture of *p*HBA and the same 7 coformers. However, would the presence of excess coformer push the disintegration of TP·*p*HBA to completion? Competition and selectivity experiments addressing this question were conducted with two selected coformers, namely MLM and ACA.

Grinding TP·*p*HBA with excess MLM results in disintegration of TP·*p*HBA and the cocrystallization of *p*HBA with MLM to form MLM·*p*HBA. The existence of the latter cocrystal was confirmed by a separate experiment in which MLM and *p*HBA were ground in stoichiometric amounts, and the PXRD pattern of the resulting product was found to be different from either pure compound. Grinding TP with a stoichiometric amount of *p*HBA and excess MLM shows that TP still has higher affinity for *p*HBA and selectively forms TP·*p*HBA. Some of the excess MLM cocrystallizes with *p*HBA and forms MLM·*p*HBA. In addition, the PXRD pattern shows the presence of some TP and MLM. Scheme 1 summarizes the findings from competition and selectivity experiments involving excess MLM.

Competition and selectivity experiments involving excess ACA resulted in a mixture of TP cocrystals (TP·*p*HBA and TP·ACA),

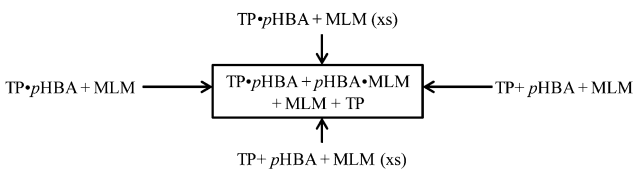

Scheme 1 Competition and selectivity experiments using equimolar and excess MLM give the same result: TP·*p*HBA disintegrates in the presence of MLM.

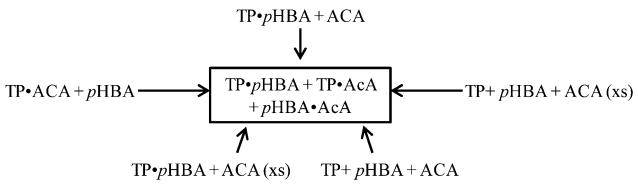

Scheme 2 Competition experiments with equimolar amount and excess ACA gave the same results as selectivity experiments involving equimolar amount and excess ACA, which were also consistent with the reverse competition experiment involving TP·ACA and *p*HBA.

as well as ACA·*p*HBA. This is the same outcome as that obtained from experiments conducted with stoichiometric amount of ACA. Scheme 2 summarizes the outcome from all reactions conducted with ACA.

Discussion

The objective of this study was to determine the robustness of TP·*p*HBA while grinding in the solid state in the presence of coformers with a variety of functional groups. The results described demonstrate that TP·*p*HBA is generally robust and maintains its integrity in the presence of a variety of functional groups including carboxylic acids, amides and phenols; however, it does disintegrate in the presence of acetamide (ACA), salicylic acid (SA), 3,5-dinitrobenzoic acid (dNBA) and melamine (MLM). In attempting to explain our results, we examined the findings in the context of the functional groups of the coformers. The intermolecular interactions sustaining TP·*p*HBA, coformers and potential cocrystals were considered since the interplay between homomeric and heteromeric interactions plays a role in cocrystal formation.[17,30]

Considering the amides, our results show that TP·*p*HBA is robust in the presence of benzamide (BZA), but it disintegrates in the presence of acetamide (ACA). Examining the crystal structure of BZA[31] (Fig. 9) reveals that it is sustained by the centrosymmetric $R_2^2(8)$ amide dimer, which further aggregates into a ladder structure, characteristic of primary amides.[32,33,34] Breaking the strong homomeric interactions in this case is difficult and unfavourable and therefore no disruption of TP·*p*HBA cocrystal is observed. The crystal structure of ACA[35] on the other hand is not sustained by the amide dimer, rather each ACA molecule interacts with 4 other molecules *via* 2 single NH···O hydrogen bonds and a bifurcated O···HN hydrogen bond. Clearly, the homomeric ACA-ACA interactions are much easier to break and therefore the heteromeric TP-ACA interactions are more likely to form.

In the case of the carboxylic acid coformers, TP·*p*HBA is robust in the presence of 4/6 coformers, but not in the presence of salicylic acid (SA) and 3,5-dinitrobenzoic acid (dNBA). Considering the relative acidity of the carboxylic acid coformers shows that SA and dNBA are the most acidic (pK_a 3.02 and 2.8, respectively)[22] and therefore the strongest hydrogen bond donors. Etter's rules[24] of hydrogen bonding dictate that the best hydrogen bond donor will interact with the best hydrogen bond acceptor. In a mixture of TP·*p*HBA and either SA or dNBA, the latter two acids are the strongest hydrogen bond donors (pK_a of *p*HBA is 4.6) and therefore likely to interact with the strongest hydrogen bond acceptor, which is the nitrogen of the imidazole ring in TP, resulting in disruption of the TP·*p*HBA cocrystal.

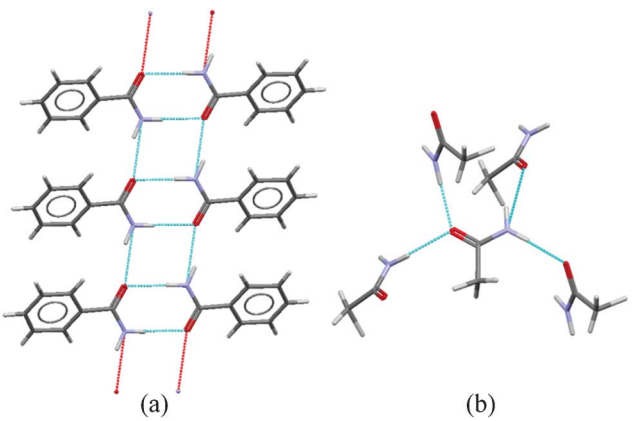

Fig. 9 Crystal structure of (a) benzamide and (b) acetamide reveals that benzamide is sustained by stronger hydrogen bonding interactions.

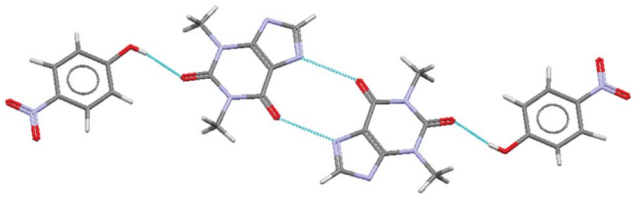

Fig. 10 Crystal structure of TP·*p*NP reveals that *p*NP interacts with TP *via* a single hydrogen bond, OH···O (CSD refcode TOPPNP).

As for the phenols, they are unable to disrupt TP·*p*HBA because the heteromeric TP-phenol interactions are likely to be weaker than the heteromeric TP-*p*HBA interactions. Examining the crystal structure of TP·*p*NP[26] (Fig. 10) clearly shows that *p*NP forms a single hydrogen bonding interaction with TP ($OH_{pNP}\cdots_{TP}O{=}C$, 2.711 Å), compared to three hydrogen bonding interactions between TP and *p*HBA (Fig. 1), ($OH_{pHBA}\cdots_{TP}O{=}C$ 2.676 Å, $C{=}O_{pHBA}\cdots_{TP}HN$ 2.729 Å and $OH_{pHBA}\cdots_{TP}N{=}C$ 2.712 Å).

Finally, TP·*p*HBA disintegrates in the presence of MLM, but no TP·MLM cocrystal is detected and trace of MLM·*p*HBA is present. MLM is sustained by very strong and extensive homomeric hydrogen bonding interactions that result in a 3D network. Such interactions are difficult to break unless favourable heteromeric interactions form, which happens with *p*HBA and not TP.

Although qualitative, plausible explanations are offered for the results observed herein, it must be stressed that additional factors, including crystal packing and lattice energy, do play a significant role in cocrystal disruption.[36]

Experimental

All chemicals were purchased from Sigma-Aldrich and used as received without further purification. Melting points were determined using a Stanford Research System EZ-melt automated melting point apparatus with digital image processing technology at a heating rate of 2 °C min^{-1}. NMR spectra (^1H and ^{13}C) were collected on a Varian Gemini 300 MHz. IR spectra were collected on a Perkin Elmer Spectrum-RX FT-IR over a range of 4000–400 cm^{-1}. DSC data were collected using a Perkin Elmer Pyris 6 using sealed 30 μL aluminium pans and an empty reference pan sealed in the same way as the sample under inert nitrogen conditions (flow rate of 30 ml min^{-1}) with a heating rate of 10 °C min^{-1} from 25 °C to 350 °C.

Powder X-ray diffraction. Data were collected on a Bruker D8 Focus X-ray powder diffractometer using Cu-Kα radiation (λ = 1.5406 Å); 40 kV and 40 mA over an angle range of 5–40° 2θ in locked coupled scan mode using a step size of 0.02 and a scan rate of 1 step/s. Mercury 2.4 was used to calculate PXRD patterns for cocrystals whose single crystal X-ray structures were previously determined. The PXRD pattern for each chemical

was determined before and after 20 min SDG with EtOH to determine if a polymorphic transition occurs. Polymorphic transitions were observed for *m*HBA, dMABA and dNBA.

Single crystal X-ray diffraction. Data were collected using a Bruker SMART APEX CCD diffractometer with monochromatized Mo-Kα radiation (λ = 0.71073 Å) connected to a KRYOFLEX low temperature device. Data were collected at 100 K. Lattice parameters were determined from least-squares analysis and reflection parameters were integrated using SAINT. Structure was solved using SHELX-97 package. All non-hydrogen atoms were refined anisotropically. All hydrogen atoms bonded to carbon, nitrogen and oxygen atoms were placed geometrically and refined with an isotropic displacement parameter fixed at $1.2U_q$ of the atoms to which they were attached.

SDG experiments. Each experiment was conducted in a 2.5 mL stainless steel grinding jar equipped with one 6.25 mm stainless steel grinding ball using a SPEX SamplePrep 8000 M Mixer/Mill at a rate of 60 Hz.

Competition experiments. In a typical experiment, TP·*p*HBA (175 mg, 0.550 mmol) was combined with equimolar amount of coformer and EtOH (0.2 μL mg^{-1}) and ground in the mixer/mill. The reaction mixture was sampled at 20, 40 and 60 min.

Selectivity experiments. In a typical experiment, stoichiometric ratio of TP (100 mg, 0.555), *p*HBA (76.7 mg, 0.555 mmol) and a coformer were combined along with EtOH (0.2 μL mg^{-1}) and ground in the mixer/mill. The reaction mixture was sampled after 20, 40 and 60 min.

Experiments involving melamine (MLM). Since the TP·MLM cocrystal is a DMSO-solvate, two sets of SDG experiments involving MLM were performed: one with EtOH (0.2 μL mg^{-1}) and one with DMSO (0.04 μL mg^{-1}). There was no noticeable difference in the outcome of the two experiments, except for the low crystallinity of the product obtained with DMSO.

SDG of individual coformers. Each coformer (*ca.* 200 mg) was independently ground with EtOH (0.2 μL mg^{-1}) to determine if a polymorphic change occurs. Polymorphic changes occurred for *m*HBA, dMABA and *p*NBA, all other coformers exhibited no change.

SDG of stoichiometric amount of *p*HBA and coformer. A stoichiometric binary mixture of *p*HBA and each of the coformers (total mass *ca.* 200 mg) was ground along with EtOH (0.2 μL mg^{-1}) for 20 min to determine if a new phase forms.

Solution crystallizations

Synthesis of TP·*p*HBA·SA. Theophylline (65 mg, 0.361 mmol), *p*HBA (50 mg, 0.362 mmol) and SA (50 mg, 0.362 mmol) were dissolved in 20 mL, 10 mL and 15 mL of water–EtOH (1 : 2), respectively. Heat was needed for complete dissolution. The clear solutions were combined and left to slow evaporate. Clear microcrystals formed within *ca.* 2 weeks.

Synthesis of TP·ACA. A binary mixture of acetamide (32.82 mg, 0.555 mmol) and theophylline (100 mg, 0.555 mmol) was SDG with EtOH (0.2 μL mg^{-1}) for 20 min. Vapour diffusion of toluene into an ethyl acetate solution of the ground product yielded microcrystalline material that was identified as TP·ACA. ^{1}H NMR (300 MHz, DMSO-d$_6$) δ (ppm) 13.61 (s, 1H, H–N$_{TP}$), 8.08 (s, 1H, H–C=), 7.32 (s, 1H, H–N$_{ACA}$), 6.73 (s, 1H, H–N$_{ACA}$), 3.49 (s, 3H, CH$_3$), 3.28 (s, 3H, CH$_3$), 1.80 (s, 3H). IR (KBr pellet) ν/cm^{-1} 3357 (N–H, s), 3298 (N–H, s), 3173 (N–H, s), 1670 (C=O, s), 1652 (C=O, s), 1564 (C=O,s); DSC melt endotherm at 269 °C.

Synthesis of TP·MLM·DMSO. Melamine (138.3 mg, 1.10 mmol) was combined with theophylline (198.6 mg, 1.10 mmol) and dissolved in 20 ml of a DMSO–water (7 : 3) solution. The vial was heated to 70° until both components dissolved. The clear solution was left uncapped and crystals formed within 2 days. ^{1}H NMR (300 MHz, DMSO-d$_6$) δ (ppm) 13.61 (s, 1H, H–N), 8.08 (s, 1H, H=C), 6.03 (s, 6H, H$_2$N–), 3.49 (s, 3H, CH$_3$), 3.28 (s, 3H, CH$_3$). IR (KBr pellet) ν/cm^{-1} 3090 (N–H, s), 1702 (C=O, s), 1654 (C=O, s). DSC melt endotherm at 178 °C.

Conclusions

This study examined the robustness of a pharmaceutical cocrystal (TP·*p*HBA) in the solid state during grinding with additives. We found that TP·*p*HBA is generally robust and does withstand the presence of a number of functional groups, including carboxylic acids, phenols and amides; however, it does disintegrate in some cases (4/11). The findings are significant in the context of pharmaceutical cocrystals, since a cocrystal must maintain its integrity during the formulation process while being ground with additives and excipients. It is therefore crucial that attention be paid to the nature of the excipient used as it may have an impact on the robustness of the cocrystal. Knowledge of crystal structures, crystal lattice energies and the mechanism of the reaction would provide additional insight into the factors that result in cocrystal disintegration. Studies involving quantitative analysis of cocrystal mixtures and crystal structure determination of ternary products are currently underway.

References

1 S. G. Fleischman, S. S. Kuduva, J. A. McMahon, B. Moulton, R. D. B. Walsh, N. Rodríguez-Hornedo and M. J. Zaworotko, *Cryst. Growth Des.*, 2003, **3**, 909–919.
2 Ö. Almarsson and M. J. Zaworotko, *Chem. Commun.*, 2004, 1889–1896.
3 D. J. Good and N. Rodriíguez-Hornedo, *Cryst. Growth Des.*, 2009, **9**, 2252–2264.
4 J. F. Remenar, S. L. Morissette, M. L. Peterson, B. Moulton, J. M. MacPhee, H. R. Guzmán and Ö. Almarsson, *J. Am. Chem. Soc.*, 2003, **125**, 8456–8457.
5 D. P. McNamara, S. L. Childs, J. Giordano, A. Iarriccio, J. Cassidy, M. S. Shet, R. Mannion, E. O'Donnell and A. Park, *Pharm. Res.*, 2006, **23**, 1888–1897.
6 D. J. Good and N. Rodríguez-Hornedo, *Cryst. Growth Des.*, 2010, **10**, 1028–1032.
7 C. B. Aakeröy, S. Forbes and J. Desper, *J. Am. Chem. Soc.*, 2009, **131**, 17048–17049.
8 H. D. Clarke, K. K. Arora, H. Bass, P. Kavuru, T. T. Ong, T. Pujari, L. Wojtas and M. J. Zaworotko, *Cryst. Growth Des.*, 2010, **10**, 2152–2167.
9 A. V. Trask, W. Motherwell and W. Jones, *Int. J. Pharm.*, 2006, **320**, 114–123.

10 A. V. Trask, W. D. S. Motherwell and W. Jones, *Cryst. Growth Des.*, 2005, **5**, 1013–1021.
11 S. Karki, T. Friščić, L. Fábián, P. R. Laity, G. M. Day and W. Jones, *Adv. Mater.*, 2009, **21**, 3905–3909.
12 R. D. B. Walsh, M. Bradner, S. Fleischman, L. Morales, B. Moulton, N. Rodriguez-Hornedo and M. Zaworotko, *Chem. Commun.*, 2003, 186–187.
13 D. Braga, E. Dichiarante, G. Palladino, F. Grepioni, M. R. Chierotti, R. Gobetto and L. Pellegrino, *CrystEngComm*, 2010, **12**, 3534–3536.
14 N. Schultheiss and A. Newman, *Cryst. Growth Des.*, 2009, **9**, 2950–2967.
15 A. V. Trask, *Mol. Pharm.*, 2007, **4**, 301–309.
16 N. Shan and M. J. Zaworotko, *Drug Discovery Today*, 2008, **13**, 440–446.
17 M. R. Caira, L. R. Nassimbeni and A. F. Wildervanck, *J. Chem. Soc., Perkin Trans. 2*, 1995, 2213–2216.
18 A. Delori, T. Friščić and W. Jones, *CrystEngComm*, 2012, **14**, 2350–2362.
19 D. R. Weyna, T. Shattock, P. Vishweshwar and M. J. Zaworotko, *Cryst. Growth Des.*, 2009, **9**, 1106–1123.
20 N. Shan, F. Toda and W. Jones, *Chem. Commun.*, 2002, 2372–2373.
21 T. Friščić, L. Fábián, J. C. Burley, W. Jones and W. D. S. Motherwell, *Chem. Commun.*, 2006, 5009–5011.
22 S. L. Childs, G. P. Stahly and A. Park, *Mol. Pharm.*, 2007, **4**, 323–338.
23 G. R. Desiraju, *Angew. Chem., Int. Ed. Engl.*, 1995, **34**, 2311–2327.
24 M. C. Etter, *Acc. Chem. Res.*, 1990, **23**, 120–126.
25 M. Sekiya, T. Yoshino, H. Tanaka and Y. Ishido, *Bull. Chem. Soc. Jpn.*, 1973, **46**, 556–561.
26 K. Aoki, T. Ichikawa, Y. Koinuma and Y. Iitaka, *Acta Crystallogr., Sect. B: Struct. Crystallogr. Cryst. Chem.*, 1978, **34**, 2333–2336.
27 N. Shan and W. Jones, *Green Chem.*, 2003, **5**, 728–730.
28 T. Friščić, A. V. Trask, W. Jones and W. Motherwell, *Angew. Chem.*, 2006, **118**, 7708–7712.
29 T. Friščić, A. V. Trask, W. Motherwell and W. Jones, *Cryst. Growth Des.*, 2008, **8**, 1605–1609.
30 C. B. Aakeröy, A. Rajbanshi, Z. J. Li and J. Desper, *CrystEngComm*, 2010, **12**, 4231–4239.
31 C. C. F. Blake and R. Small, *Acta Crystallogr., Sect. B: Struct. Crystallogr. Cryst. Chem.*, 1972, **28**, 2201–2206.
32 L. Leiserowitz and A. Hagler, *Proc. R. Soc. London, Ser. A*, 1983, **388**, 133–175.
33 S. S. Kuduva, D. Bläser, R. Boese and G. R. Desiraju, *J. Org. Chem.*, 2001, **66**, 1621–1626.
34 C. B. Aakeröy, B. M. T. Scott and J. Desper, *New J. Chem.*, 2007, **31**, 2044–2051.
35 W. Denne and R. Small, *Acta Crystallogr., Sect. B: Struct. Crystallogr. Cryst. Chem.*, 1971, **27**, 1094–1098.
36 N. Schultheiss, M. Roe and S. X. M. Boerrigter, *CrystEngComm*, 2011, **13**, 611–619.